Effects of A1 site occupation on dielectric and ferroelectric properties of $Sr_4CaRTi_3Nb_7O_{30}$ (R = Ce, Eu) tungsten bronze ceramics*

Fang Yu-Jiao(方玉娇), Gong Gao-Shang(龚高尚), Gebru Zerihun, and Yuan Song-Liu(袁松柳)†

School of Physics, Huazhong University of Science and Technology (HUST), Wuhan 430074, *China*

(Received 22 May 2014; revised manuscript received 25 June 2014; published online 10 October 2014)

$Sr_4CaRTi_3Nb_7O_{30}$ (R = Ce, Eu) tungsten bronze ceramics are prepared by a standard solid state reaction method. The effects of A1 site occupation on the dielectric and ferroelectric properties of $Sr_4CaRTi_3Nb_7O_{30}$ (R = Ce, Eu) tetragonal tungsten bronzes are investigated. The $Sr_4CaCeTi3Nb_7O_{30}$ shows a normal transition behavior due to the closer size ion occupation in A1 sites, which could suppress the distortion of B2 octahedra effectively. $Sr_4CaEuTi_3Nb_7O_{30}$ ceramic exhibits two dielectric anomalies, which might be related to the fact that the large radius difference between Ca^{2+} and Eu^{3+} could lead to the uneven distribution of Ca^{2+} and Eu^{3+} in A1 sites and form two slightly different kinds of compositions with different transition temperatures in the structure. Our results indicate that the ionic radius difference in A1 sites plays an important role in determining the dielectric and ferroelectric natures of the filled tungsten bronze ceramics. Polarization–electric field (P–E) curves are evaluated at room temperature and both of them show hysteresis loops. $Sr_4CaCeTi_3Nb_7O_{30}$ shows a fat hysteresis loop, indicating the long-range ferroelectric order in the ceramic. The current density–electric field (J–E) curves are measured at room temperature with a largest leakage current density of $\sim 10^{-6}$ A/cm^2, indicating that their leakage currents are rather low.

Keywords: dielectric anomaly, relaxation, ferroelectricity

PACS: 87.19.rf, 31.70.Hq, 77.84.–s **DOI:** 10.1088/1674-1056/23/12/128701

1. Introduction

The filled tetragonal tungsten bronze structure consists of a complex array of distorted BO_6 octahedra sharing corners in such a way that two types of interstices pentagonal A1, square A2 can be occupied by cations, which results in a general formula $(A1)_2(A2)_4(B1)_2(B2)_8O_{30}$.[1] Generally, site A2 is occupied by Ba or Sr, and A1 is occupied by alkaline earth and rare earth cations, resulting in the formulas of $M_4R_2Ti_4Nb_6O_{30}$ and $M_5RTi_3Nb_7O_{30}$.[2–11] Owing to the complex dielectric, ferroelectric properties, and their possible applications in electronic devices, the filled tetragonal tungsten bronze ceramics have received much scientific attention of researchers in recent years.[2–16] The previous work suggested that the ion radius of A1 and A2 sites especially the difference between them (ΔR) as the dominant parameter that governs the dielectric nature.[17] That is, ceramics with larger ΔR tend to show a normal ferroelectric transition and those with smaller ΔR are expected to be relaxor ferroelectric materials.[17] For example, $Ba_4La_2Ti_4Nb_6O_{30}$,[18] $Ba_5LaTi_3Nb_7O_{30}$,[9] $Sr_5SmTi_3Nb_7O_{30}$,[19] and $Sr_5LaTi_3Nb_7O_{30}$[20] ceramics tend to be relaxor ferroelectric materials, and $Ba_4Nd_2Ti_4Nb_6O_{30}$,[2,4,21] $Ba_4Sm_2Ti_4Nb_6O_{30}$,[6] and $Sr_4Sm_2Ti_4Nb_6O_{30}$[7] exhibit normal ferroelectric transitions. However, how different sizes of ion occupation in A1-sites affect the ferroelectric nature is rarely reported. The previous published papers of $M_5RTi_3Nb_7O_{30}$ ceramics show that site A2 is generally occupied by Ba or Sr, and R is occupied by rare earth cations. However, Ba^{2+}/Sr^{2+} always possesses a larger ion radius than rare earth elements, so it is difficult to investigate how the cations occupation in A1-sites affect the dielectric and ferroelectric natures in $M_5RTi_3Nb_7O_{30}$. Noticing that the alkaline earth element Ca^{2+} possesses an ion radius comparable to rare earth cations. Substituting Ca^{2+} for one Ba^{2+}or Sr^{2+} in site A1 may provide us with the possibility to explore how the ions size difference in A1-sites affects the dielectric properties effectively.

In the present work, we choose Ca to substitute Sr at the A1 site, and for rare earth elements, we choose Ce and Eu. $R(Ce^{3+})$ = 0.102 nm, which is slightly larger than Ca^{2+} [$R(Ca^{2+})$ = 0.100 nm] in size. While Eu possesses a smaller ion radius than Ca, that is, $R(Eu^{3+})$ = 0.0947 nm. Thus we may explore how the A1 site ion size influences the dielectric and ferroelectric properties of the filled tetragonal tungsten bronze ceramic accurately. Therefore, in the present work, the $Sr_4CaRTi_3Nb_7O_{30}$ (R = Ce, Eu) tungsten bronze ceramics in which A1 sites are occupied by Ca and R are investigated. How the ion radius difference in site A1 affects the dielectric anomalies is investigated. Their ferroelectric properties have also been probed.

*Project supported by the National Natural Science Foundation of China (Grant No. 11174092) and the Key Project of Henan Provincial Educational Committee, China (Grant No. 14A140019).

†Corresponding author. E-mail: yuansl@hust.edu.cn

© 2014 Chinese Physical Society and IOP Publishing Ltd

2. Experiment

$Sr_4CaCeTi_3Nb_7O_{30}$ and $Sr_4CaEuTi_3Nb_7O_{30}$ ceramics were prepared by the conventional solid-state reaction and sintering process. The weighed raw materials were ground for 8 h and calcinated in a high-purity alumina crucible at 1100 °C in air for 3 h followed by a second grinding to reach a homogeneous granulometric distribution. The reground powder was pressed into cylindrical disks each 12 mm in diameter and 1 mm in thickness under a pressure of 30 MPa. The disks were sintered at 1300 °C for 3 h. After this process, the ceramics were slowly cooled to 1100 °C at a rate of 2 °C/min and then cooled down naturally. The crystal structures of the samples were examined by X-ray diffraction (XRD) using Cu Kα radiation (Philips X-ray diffractometer). For electrical properties measurements, electrodes were attached to both surfaces of the disk with silver paste. To determine the dielectric constant, dielectric loss, and their dependences on frequency, the dielectric properties were measured in wide temperature and frequency ranges by using a Wayne Kerr 6500B precision impedance analyzer. The ferroelectric hysteresis loops (P–E) and leakage currents were evaluated at room temperature by a standard ferroelectric tester (Precision Premier II, Radiant Technology).

3. Results and discussion

In Fig. 1 we show X-ray diffraction patterns of $Sr_4CaCeTi_3Nb_7O_{30}$ and $Sr_4CaEuTi_3Nb_7O_{30}$ ceramics. The tetragonal tungsten bronze structures in space group $P4bm$ are determined. A small amount of impurity phase is detected and asterisked in the figure.

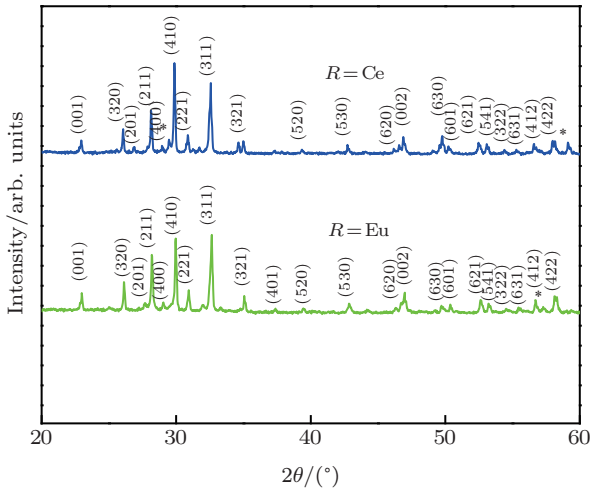


Fig. 1. (color online) XRD patterns of the $Sr_4CaRTi_3Nb_7O_{30}$ (R = Ce, Eu) ceramics.

Figures 2(a) and 2(b) show the dielectric properties of $Sr_4CaCeTi_3Nb_7O_{30}$ and $Sr_4CaEuTi_3Nb_7O_{30}$ ceramics respectively. A slight anomaly appears at 260 °C for $Sr_4CaCeTi_3Nb_7O_{30}$ at low frequency. However, after the second high temperature measurement, it vanishes at high frequency as can be seen in the inset of Fig. 2(a), which might be due to the surface effect of the silver paste. $Sr_4CaCeTi_3Nb_7O_{30}$ shows only one dielectric peak at ∼ 103 °C, while $Sr_4CaEuTi_3Nb_7O_{30}$ ceramics exhibit two dielectric anomalies at ∼ 100 °C and ∼ 250 °C respectively. This might be related to the fact that in $Sr_4CaCeTi_3Nb_7O_{30}$, there is almost no radius difference in A1 sites due to the close ionic radii of Ca^{2+} and Ce^{3+}. Thus Ca^{2+} and Ce^{3+} can distribute homogenously in A1 sites, which leads to only one ferroelectric transition, while the large radius difference between Ca^{2+} and Eu^{3+} cations leads to the uneven distributions of Ca^{2+} and Eu^{3+} in A1 sites. Thus for $Sr_4CaEuTi_3Nb_7O_{30}$ ceramic, the inhomogeneous micro-composition in the structure results in two different kinds of ferroelectric domains with different transition temperatures.

The dielectric peaks in Fig. 2(a) indicate the normal ferroelectric transition for $Sr_4CaCeTi_3Nb_7O_{30}$. While $Sr_4CaEuTi_3Nb_7O_{30}$ exhibits a normal ferroelectric transition at a higher temperature, together with a dielectric relaxation at lower temperature, despite the fact that $Sr_4CaCeTi_3Nb_7O_{30}$ possesses smaller ΔR and is expected to show relaxation according to the ΔR theory.[14] The normal ferroelectric peak in $Sr_4CaCeTi_3Nb_7O_{30}$ may be explained as follows. In a displacive type ferroelectric, the central cation displacement is sensitive to the distortion of the octahedron. The lattice distortion exerts the effect on the correlation of polar cation displacement, which could finally hinder long-range dipolar coupling and give rise to the polar nano-regions.[22–24] The closer ionic radius occupations of Ca and Ce in A1-sites suppress the disturbing of ferroelectric ordering by suppressing Ti/Nb(2)O_6 octahedral distortion significantly,[22] which results in the formation of a long-range ferroelectric order. Thus a normal ferroelectric transition shows up. For $Sr_4CaEuTi_3Nb_7O_{30}$, Ca^{2+} and Eu^{3+} distribute inhomogeneously, which leads to two different micro-compositions in the structure. The relaxation anomaly may be explained as follows. The anomaly, caused by the composition that contains more Ca^{2+} ions, can be confirmed as it appears at ∼ 100 °C, which is quite similar to the transition temperature of $Sr_4CaCeTi_3Nb_7O_{30}$ (∼ 103 °C). The large ionic radius difference between Ca and Eu in A1 sites may enhance the distortion of B2 octaheral nearby. The enhanced B2 octahedral distortion hinders long-range dipolar coupling and gives rise to the formation of the polar nano-regions. Thus the relaxation anomaly emerges. The normal ferroelectric transition at higher temperature might be caused by the composition which contains more Eu^{3+} ions, thereby possessing smaller radius in A1 sites and larger radius difference between A1 and A2 sites. According to the ΔR theory, larger ΔR between A1 and A2 sites tends to show normal ferroelectric transition. From the discussion above, the conclu-

sion can be drawn that the radius difference in A1 sites exerts the same important role as ΔR theory in determining the dielectric nature of filled tungsten bronzes by affecting the ionic distribution in A1 sites and the ferroelectric order length.

The solid lines in Figs. 3(a) and 3(b) show the Curie–Weiss law fittings of the real parts of the dielectric constant for $Sr_4CaCeTi_3Nb_7O_{30}$ and $r_4CaEuTi_3Nb_7O_{30}$ at 1MHz. The permittivity curves are fitted to the Curie–Weiss relationship

$$\varepsilon' = \frac{C}{T - T_0},$$

where ε' is the real part of dielectric permittivity, T_0 is the Curie–Weiss temperature, and C is the Curie–Weiss constant. For $Sr_4CaCeTi_3Nb_7O_{30}$ and $Sr_4CaEuTi_3Nb_7O_{30}$, the values of C equal respectively. The order of magnitude confirms that it is a displacive type of ferroelectric material.

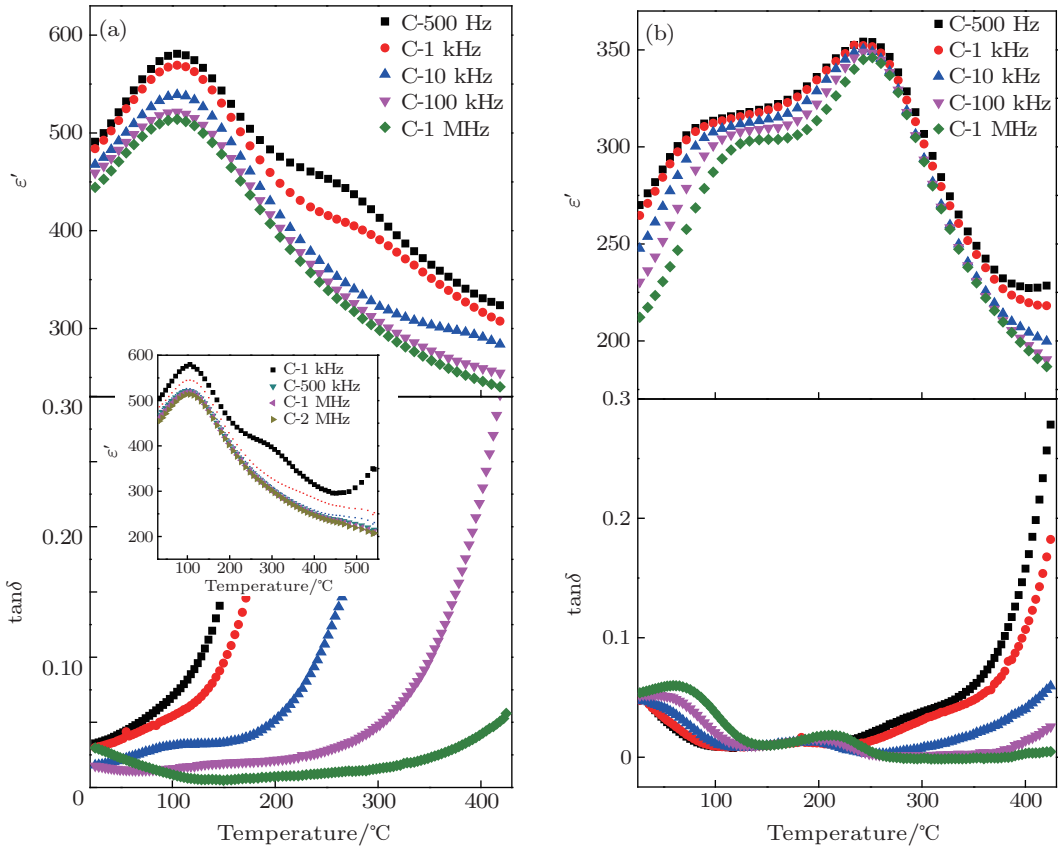


Fig. 2. (color online) Temperature dependences of real dielectric permittivity and dielectric loss tan δ at frequencies between 500 Hz and 1 MHz for (a) $Sr_4CaCeTi_3Nb_7O_{30}$ and (b) $Sr_4CaEuTi_3Nb_7O_{30}$; the inset shows the real dielectric permittivity at high frequency and temperature.

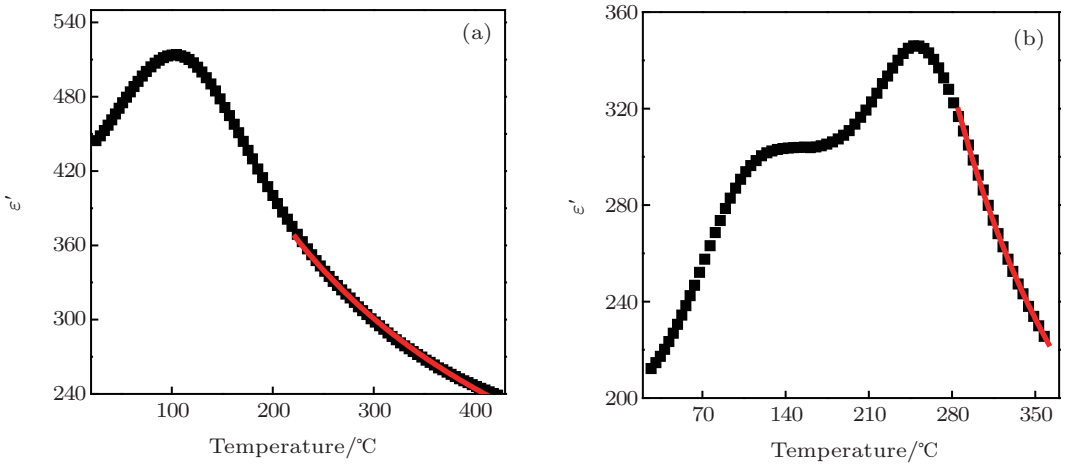


Fig. 3. (color online) Curie–Weiss law fittings of the real part of the dielectric constant for (a) $Sr_4CaCeTi_3Nb_7O_{30}$ and (b) $Sr_4CaEuTi_3Nb_7O_{30}$ at 1 MHz.

Figure 4 shows the room temperature ferroelectric hysteresis loops of the $Sr_4CaCeTi_3Nb_7O_{30}$ and $Sr_4CaEuTi_3Nb_7O_{30}$ ceramics. The measured values of remnant polarization ($2P_r$) for the ceramics are 2.70 μC/cm^2 and 1.12 μC/cm^2 respectively. For $Sr_4CaCeTi_3Nb_7O_{30}$, a fat hysteresis loop is obtained, suggesting the ferroelectric nature of long-range ferroelectric order.[25] For $Sr_4CaEuTi_3Nb_7O_{30}$, lanky nonlinear loops could be observed, indicating the weak room temperature ferroelectricity. This might also be due to the fact that the closer ionic radius occupations of Ca^{2+} and Ce^{3+} in A1 sites suppress the Ti/Nb(2)O6 octahedral distortion and give rise to the formation of long-range ferroelectric coupling.[22]

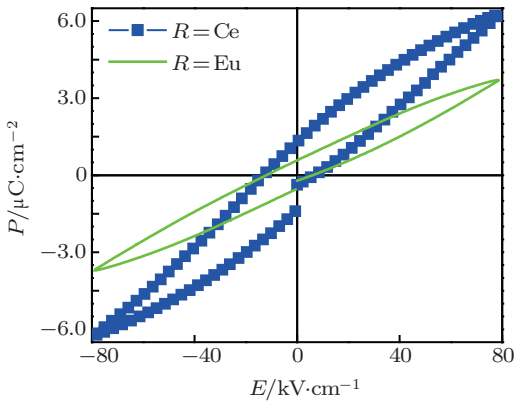


Fig. 4. (color online) Polarization–electric field (P–E) loops for the $Sr_4CaRTi_3Nb_7O_{30}$ (R = Ce, Eu) ceramics at room temperature.

Room temperature current density–electric field curves are shown in Fig. 5. All of the curves each show a low leakage current ($\sim 10^{-6}$). Compared with the $Sr_4CaEuTi_3Nb_7O_{30}$, $Sr_4CaCeTi_3Nb_7O_{30}$ exhibits a large leakage current.

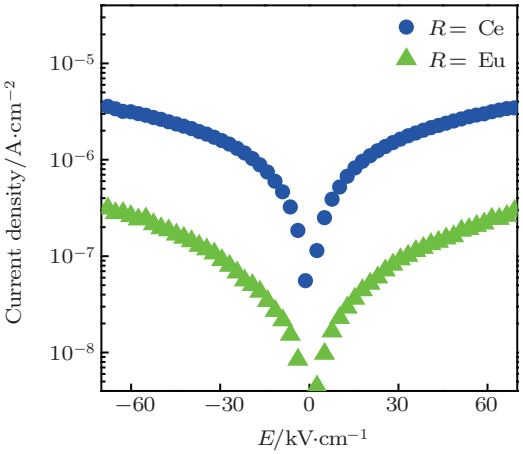


Fig. 5. (color online) Current density–electric field (J–E) curves for $Sr_4CaRTi_3Nb_7O_{30}$ (R = Ce, Eu) ceramics at room temperature.

4. Conclusion

The tetragonal tungsten bronze structures in space group $P4bm$ are determined in $Sr_4CaRTi_3Nb_7O_{30}$ (R = Ce, Eu) ceramics. The dielectric and ferroelectric properties are investigated together with their crystal structure. A normal ferroelectric transition is revealed in $Sr_4CaCeTi_3Nb_7O_{30}$, which may be attributed to the homogeneous and ordered structure formed in the ceramic. $Sr_4CaEuTi_3Nb_7O_{30}$ is found to exhibit relaxation at lower temperature, together with a normal ferroelectric transition at a higher temperature. Our results indicate that an ionic radius difference in A1 sites may affect the distribution of A1 site ions and the ferroelectric order length seriously, which plays an important role in determining the dielectric nature of the tetragonal tungsten bronze ceramic. Owing to the long-range ferroelectric order, $Sr_4CaCeTi_3Nb_7O_{30}$ shows a strong room temperature ferroelectric property. The J–E curves indicate that the leakage current for both of them are low.

Acknowledgment

We would like to thank the colleagues of the Analysis Center of HUST for their assistance in various measurements.

References

[1] Parida B N and Das P R 2014 *J. Alloys Compd.* **585** 234
[2] Stennett M C, Reaney I M, Miles G C, Woodward D I, West A R, Kirk C A and Levin I 2007 *J. Appl. Phys.* **101** 104114
[3] Prades M, Beltrań H, Maso Ń, Cordoncillo E and West A R 2008 *J. Appl. Phys.* **104** 104118
[4] Zhu X L, Wu S Y and Chen X M 2007 *Appl. Phys. Lett.* **91** 162906
[5] Zhu X L and Chen X M 2010 *Appl. Phys. Lett.* **96** 032901
[6] Zheng X H and Chen X M 2003 *Solid State Commun.* **125** 449
[7] Sun Y H, Chen X M and Zheng X H 2004 *J. Appl. Phys.* **96** 7435
[8] Zhu X L, Liu X Q and Chen X M 2011 *J. Am. Ceram. Soc.* **94** 1829
[9] Li K, Zhu X L, Liu X Q and Chen X M 2012 *Appl. Phys. Lett.* **100** 012902
[10] Kirk C A, Stennett M C, Reaney I M and West A R 2002 *J. Mater. Chem.* **12** 2609
[11] Levin I, Stennett M C, Miles G C, Woodward D I, West A R and Reaney I M 2006 *Appl. Phys. Lett.* **89** 122908
[12] Zhu X L and Chen X M 2014 *Chin. Phys. Lett.* **31** 015201
[13] Song W L, Cao M S and Zhou Y 2008 *Chin. Phys. Lett.* **25** 1902
[14] Qi Y and Du A 2014 *Chin. Phys. B* **23** 087502
[15] Xu Z, Gao J J, Yao X, Zhang C H and Zhu C J 2011 *Chin. Phys. B* **20** 097702
[16] Uzma G 2014 *Chin. Phys. B* **23** 057502
[17] Simon A and Ravez J 2006 *C. R. Chim.* **9** 1268
[18] Kirk C A, Stennett M C, Reaney I M and West A R 2002 *J. Mater. Chem.* **12** 2609
[19] Sun Y H, Chen X M and Zheng X H 2004 *J. Appl. Phys.* **96** 7435
[20] Zhu X L, Li K, Rafiq M A, Liu X Q and Chen X M 2013 *J. Appl. Phys.* **114** 124102
[21] Kamba S, Veljko S, Kempa M, Savinov M, Bovtun V, Vaněk P, Petzelt J, Stennett M C, Reaneyand I M and West A R 2005 *J. Eur. Ceram. Soc.* **25** 3069
[22] Li K, Zhu X L, Liu X Q and Chen X M 2012 *Appl. Phys. Lett.* **101** 042906
[23] Maier B, Mihailova B, Paulmann C, Ihringer J, Gospodinov M, Stosch R, Güttler B and Bismayer U 2009 *Phys. Rev. B* **79** 224108
[24] Laulhe C, Pasturel A, Hippert F and Kreisel J 2010 *Phys. Rev. B* **82** 132102
[25] Li K, Zhu X L, Liu X Q and Chen X M 2013 *J. Appl. Phys.* **114** 044106